Lung disease severity, Coronary Artery Calcium, Coronary inflammation and Mortality in Coronavirus Disease 2019

Nicola Gaibazzi[1], Chiara Martini[2], Maria Mattioli[1], Domenico Tuttolomondo[1], Angela Guidorossi[1], Sergio Suma[1], Damini Dey[3], Anselmo Palumbo [2], Massimo De Filippo[2]

Azienda Ospedaliero-Universitaria di Parma, Parma, Italy

Author position, institution and location

Nicola Gaibazzi MD, Cardiology Department, Azienda Ospedaliero-Universitaria di Parma, Parma Italy

Chiara Martini RT, Radiology Department, Azienda Ospedaliero-Universitaria di Parma, Parma Italy

Maria Mattioli MD, Cardiology Department, Azienda Ospedaliero-Universitaria di Parma, Parma Italy

Domenico Tuttolomondo MD, Cardiology Department, Azienda Ospedaliero-Universitaria di Parma, Parma Italy

Angela Guidorossi MD, Cardiology Department, Azienda Ospedaliero-Universitaria di Parma, Parma Italy

Sergio Suma MD, Cardiology Department, Azienda Ospedaliero-Universitaria di Parma, Parma Italy

Damini Dey PhD, Biomedical Imaging Research Institute, Department of Biomedical Sciences, Cedars-Sinai Medical Center, Los Angeles, 90048, USA

Anselmo Palumbo, MD, Radiology Department, Azienda Ospedaliero-Universitaria di Parma, Parma Italy

Massimo De Filippo MD, Radiology Department, Azienda Ospedaliero-Universitaria di Parma, Parma Italy

[1] Cardiology Department and [2] Radiology Department, Azienda Ospedaliero-Universitaria di Parma, Parma Italy, [3] Biomedical Imaging Research Institute, Department of Biomedical Sciences, Cedars-Sinai Medical Center, Los Angeles, 90048, USA.

Corresponding Author: Nicola Gaibazzi, MD, UOC di Cardiologia, Coordinamento attività specialistiche ambulatoriali cardiologiche, Azienda Ospedaliero-Universitaria di Parma, Via Gramsci 14, 43126, Parma, Italy.

E-mail ngaibazzi@ao.pr.it)

Telephone number: +39 0521 704962.

Fax number: +39 0521 702189.

Conflicts of interest: All authors have nothing to disclose regarding this manuscript. Outside the current manuscript, Dr. Dey may receive software licensing royalties from Cedars-Sinai Medical Center.

Authors' contribution: Dr Gaibazzi, wrote the manuscript with the assistance of Dr Mattioli, Dr Dey, Dr Guidorossi and Dr Tuttolomondo. Dr Chiara Martini collected most of the CT

data and Dr Gaibazzi and Dr Dey were responsible for the database integrity as well as the statistical analysis required. All authors have read and approved the revised manuscript.

Word count: 4859.

Abstract

Aims. The in-hospital mortality rate of the coronavirus disease 2019 (COVID-19) is higher in case of myocardial injury, but the underlying mechanism is unknown. We conducted a study on COVID-19 patients to determine the association of the extent of lung disease or coronary artery chest computed tomography (HRCT) variables, the Agatston coronary calcium score (CCS) and peri-coronary adipose tissue (PCAT) attenuation, with mortality.

Methods and results. A single-center retrospective case series of 500 consecutive patients was collected, with chest HRCT performed as a gatekeeping-strategy in the workup of patients admitted for suspected COVID-19 to our emergency department in Northern Italy, from March 5 to March 15, 2020. Patients with laboratory-confirmed COVID-19 formed the final study group. The endpoint was in-hospital mortality at the time of final follow-up (March 30, 2020). Demographic, clinical, laboratory and HRCT data were collected from hospital electronic records, and HRCT features (CCS and PCAT attenuation) were measured post-hoc from HRCT images.

Among 500 patients with suspected COVID-19, 279 had laboratory-confirmed COVID-19 and formed the study group. Among them, 170 patients (61%) were discharged alive and 109 (39%) died. Comparing patients discharged alive with patients who died, the median age was 65 vs 77 ($p<0.001$), with males 56% vs 68% ($p=0.061$), prior cardiovascular disease 9% vs 24% ($p=0.001$), median D-dimer 723 vs 1083 ng/ml ($p<0.001$), median C-reactive protein 78 vs 148 mg/L ($p<0.001$), the mean CCS 17 vs 189 ($p<0.001$) and the median PCAT attenuation -76.4 HU vs -68.6 HU ($p<0.001$). In multivariable analysis, only age ($p<0.001$), D-dimer ($p=0.041$), C-reactive protein ($p=0.002$), HRCT lung disease extent ($p=0.002$) and peri-coronary adipose tissue attenuation ($p<0.001$) – not the Agatston CCS – were independently associated with mortality.

Conclusions. Our study suggests that higher mortality in COVID-19 may be at least partly mediated by coronary artery inflammation, rather than subclinical coronary artery disease extent.

Key words: COVID-19 – coronary calcium score - coronary adipose tissue attenuation – coronary inflammation – high-resolution computed tomography

List of abbreviations

CAD	coronary artery disease
CCS	coronary calcium score
COVID-19	coronavirus disease 2019
CRP	C-reactive protein
HRCT	high resolution computed tomography
HU	Hounsfield Units
LAD	left anterior descending coronary artery
PCAT	peri-coronary adipose tissue
RT-PCR	real time - polymerase chain reaction
SARS-CoV-2	severe acute respiratory syndrome coronavirus 2

Introduction

Coronavirus disease 2019 (COVID-19) has spread rapidly in the North of Italy, the European Country with the highest number of COVID-19 related deaths. Individuals with the highest mortality are typically older, with underlying comorbidities, often cardiovascular disease. (1-3) Recent studies have reported that 15% to 30% of hospitalized COVID-19 patients are diagnosed with acute myocardial injury, based on increased cardiac troponins, and their mortality is increased (4-6). The demonstration of an association between myocardial injury and mortality in COVID-19 is key, but it does not reveal the underlying mechanism. This may include supply/demand imbalance ischemia, due to hypoxemia, or disruption of coronary plaques by acute inflammation, or also direct viral infection of the myocardium (7,8).

In our centre, a diagnostic strategy based on gatekeeping high-resolution computed tomography of the chest (HRCT) was set in place to overcome the long delays initially required by overloaded labs to provide the results of nasopharyngeal swabs. Patients showing respiratory distress or history of fever/dry cough and reduced O_2 saturation were fast-tracked to HRCT from the dedicated COVID-19 triage. Patients with HRCT findings compatible with COVID-19 were admitted to dedicated wards, where treatment was started, while waiting for diagnostic confirmation by severe acute respiratory syndrome - coronavirus 2 (SARS-CoV-2) real-time reverse transcriptase–polymerase chain reaction (RT-PCR) assay.

We aimed to investigate whether the Agatston coronary calcium score (CCS), which correlates with coronary artery disease (CAD) (9), or peri-coronary adipose tissue (PCAT) attenuation, which correlates with coronary inflammation (10), are associated with higher mortality in COVID-19 patients, independently from other risk factors and extent of lung disease. Both

parameters can be measured in HRCT scans, although only CCS has been previously measured in non-contrast, non ECG-triggered HRCT scans (11). This would suggest either a prevailing role of pre-existing CAD, leading to supply/demand imbalance, or plaque disruption promoted by coronary inflammation as possible mechanisms determining a worse outcome in COVID-19. This study describes consecutive patients from a single academic centre involved in the early COVID-19 outbreak and examines the potential association between the lung disease extent, CCS and PCAT attenuation measured on HRCT and mortality in patients with COVID-19 confirmed by SARS-CoV-2 RT-PCR assay (12).

Methods

This retrospective, single-centre, observational case series study was performed at the Parma University Hospital, Parma, Italy, which has been designated to treat patients with COVID-19 in this area in the North of Italy, serving slightly less than half-million citizens.

The first consecutive 500 patients, who presented at the dedicated hospital triage with clinically suspected COVID-19, between March 05, 2020 and March 15, 2020, and were indicated for fast-track HRCT were first selected; the subgroup of such patients who subsequently had SARS-CoV-2 viral nucleic acid detected in nasopharyngeal swabs formed the final study group. (12) This group was analyzed to evaluate the association of independent variables with in-hospital mortality.

Definition of clinically suspected COVID-19

Clinical variables considered at triage to define "clinically suspected COVID-19" were a) recent/current fever for at least 2 days, b) dry cough, c) respiratory distress during mild exercise or at rest. O_2 saturation<96% (<94% for patients with chronic pulmonary disease) using pulse oximetry was defined reduced O_2 saturation. The presence of at least one of the abovementioned

clinical criteria + reduced O_2 saturation qualified the subject as clinically suspected COVID-19 and mandated fast-track HRCT, as the gatekeeper to admit patients to dedicated COVID-19 wards if showing interstitial pneumonia, even if SARS-CoV-2 viral nucleic acid laboratory results were pending. All patients were admitted to hospital after HRCT, either to COVID-19 specialized or general wards, based on the presence or absence of HRCT findings suggestive of COVID-19 pneumonia.

Definition of laboratory-confirmed COVID-19

The detection of SARS-CoV-2 viral nucleic acid in nasopharyngeal swabs was used as the only reference to adjudicate laboratory-confirmed COVID-19. This study complied with the edicts of the 1975 Declaration of Helsinki and was approved by the institutional ethics board of Parma University Hospital with expedited approval for COVID-19 studies (371/2020/OSS/AOUPR). Written informed consent was waived by the ethics commission due to the emergency state caused by COVID-19.

Data Collection

The electronic discharge letter and other available hospital electronic records were reviewed by a team of physicians working in Parma University Hospital. Clinical and laboratory information was collected on admission and during hospitalization by attending physicians and was then checked and recorded by the researchers. Patient data including demographics, medical history, comorbidities, available laboratory examinations, nasopharyngeal swabs tested with SARS-CoV-2 RT-PCR assay, or other intensive care measures and outcomes were collected.

High-resolution computed tomography

Patients were scanned with a 128-slice Somatom Definition Edge scanner (Siemens Medical Solutions, Forchheim, Germany), equipped with an integrated high-resolution circuit detector.

Examinations were performed with patients in supine position, at full inspiration, without the use of contrast medium. Scan parameters were: collimation 128×0.6 mm; rotation time 0.33 ms; pitch 1.2; tube voltage 120 kVp; tube power 150 reference mAs; tube current modulation on. Scan data were reconstructed with novel model based iterative reconstruction algorithm (ADMIRE) keeping the noise at a low level and preserving intrinsic low-contrast details.

Interpretation of HRCT

Each scan was clinically evaluated by the radiologist in charge, all having more than 10-year experience, in particular using the following classification, similar to the recent Consensus Statement by the Radiological Society of North America (13). In our centre, the three following summary categories were used: a) presence of COVID-19 typical interstitial pneumonia, according to the presence of ground-glass opacities, bilateral multifocal patchy consolidation, and/or interstitial changes with a peripheral distribution, b) indetermined appearance, in case of absence of typical features and presence of multifocal, diffuse, perihilar, or unilateral ground-glass opacities with or without consolidation lacking a specific distribution and non-rounded or non-peripheral, c) negative for pneumonia. The report also focused per-protocol on the estimated semi-quantitative percentage of lung parenchyma involved (5 visually-assessed classes, <10%, 10-19%, 20-49%, 50-79%, >80%).

Calcium scoring

Coronary calcium was classified using a threshold of 130 Hounsfield units (HU) involving 3 contiguous voxels for identification of a calcific lesion resulting in a minimum lesion area of 1.02 mm^2. The lesion score was calculated using the area density method, by multiplying the lesion area by a density factor derived from the maximal HU within the area, as described by Agatston (14). The CCS was calculated with commercially available software (CaScore; Siemens, Germany).

Peri-coronary Adipose Tissue (PCAT) Attenuation

To measure PCAT attenuation, we used a software package clinically validated for this use (AutoPlaque^{TM} Version 2.5, Cedars-Sinai Medical Center) (15). Since in the current study we used high-quality and fast HRCT machines, but the scans were not ECG-triggered nor contrast medium used, we customized the methods otherwise typically used for PCAT attenuation measurement; we manually identified the coronary artery lumen and adjusted the vessel contours. The left anterior descending coronary artery (LAD) was the only coronary artery vessel reliably visualized in most patients, due to less motion artifacts compared with right coronary artery, in the non-contrast, non ECG-triggered HRCT datasets for the aim of PCAT attenuation measurement. Figure 1 shows the technical steps to measure PCAT attenuation. We traced the proximal 40-mm segment of the LAD and 3-dimensional layers within radial distance from the outer coronary wall equal in thickness to the average diameter of the vessel were constructed automatically, using the abovementioned semiautomated software Within the predefined volume of interest, voxels with tissue attenuation ranging from -190 up to -30 HU were considered as adipose tissue. We quantified the mean PCAT attenuation based on the attenuation histogram of peri-coronary fat within the range –190 HU to –30 HU (10,15,16).

Figure 1

Outcome

The primary endpoint was incidence of in-hospital death in laboratory-confirmed COVID-19 patients. Successful clinical course leading to hospital discharge comprised relieved clinical symptoms, normal body temperature, normal O_2 saturation with no need of O_2 therapy and at least partial decrease of inflammation as shown by C-reactive protein (CRP) testing.

Statistical Analysis

No statistical sample size calculation was performed a priori, and sample size was equal to the number of patients enrolled during the study period. Categorical variables are expressed as number of patients (percentage) with 95% CIs, and continuous variables as mean (SD) or median (interquartile range [IQR]) as appropriate. The means for continuous variables were compared using independent group t tests when the data were normally distributed, otherwise, the Mann-Whitney test was used. Proportions for categorical variables were compared using the $\chi 2$ test, although the Fisher exact test was used when data were limited. Stepwise multiple logistic regression was used to assess the relationship between the demographic and clinical variables, laboratory variables and, as a final step, HRCT variables and the primary end point of death. Variables that were not normally distributed such as CCS, CRP, and D-dimer were log-transformed, as is standard. We considered an increase in PCAT attenuation in steps of 1 HU and 5 HU; the results were similar and increase by 5 HU were reported for multivariable analysis. All variables with $p<0.1$ on univariable analysis were considered for the inclusion into multivariable logistic regression models. A 2-sided $p<0.05$ was considered statistically significant. All statistical analyses were performed with Stata statistical software, version 15.0 (StataCorp LLC, USA).

Results

Suspected COVID-19 overall group (n=500)

Among the initially 500 consecutive patients with clinically-suspected COVID-19 who underwent HRCT, n=145 died (29%) during their index hospitalization, at a median of 6 (lower-upper quartile, 4-10) days after admission, while n=355 were discharged home alive after a median of 6 (lower-upper quartile, 2-13) days. n=279 (55.8%) were found positive for RT-PCR viral nucleic acid detection in the nasopharyngeal swab obtained either at presentation, or repeated in the

next 2 days if the first was negative, and they received the diagnosis of laboratory-confirmed COVID-19.

In this initial cohort n=399 patients had typical findings of COVID-19 interstitial pneumonia on HRCT, n=66 were negative for COVID-19 pneumonia and n=35 were indeterminate cases. Figure 2 shows the mortality rate in the overall n=500 population, based on HRCT findings of typicality for COVID-19, but also based on laboratory detection of SARS-CoV-2 nucleic acid in nasopharyngeal swabs. HRCT findings for COVID-19 demonstrated the following prevalence of SARS-CoV-2 nucleic acid detected in patients' nasopharyngeal swabs: 248/399 (62%) in COVID-19 typical HRCT, 19/35 (54%) in indeterminate HRCT, 12/66 (18%) in negative HRCT.

Figure 2

Figure 2 shows that the visual semi-quantitative estimate of diseased lung parenchyma, as reported by the radiologist in charge (here summarized in 3 classes, 0-19%, 20-49% and ≥50%) was associated with mortality, in laboratory-confirmed COVID-19 patients but also in patients with negative report for SARS-CoV-2 nucleic acid in the nasopharyngeal swabs.

Laboratory-confirmed COVID-19 group (n=279)

These patients with laboratory-confirmed COVID-19 formed the final study cohort, described and tested for univariable and multivariable association between demographic, laboratory, standard and novel variables on HRCT and in-hospital mortality.

In this cohort, n=170 (61%) patients were discharged home alive at a median of 8 days (lower-upper quartile, 5-16) after admission, while n=109 (39%) died during hospitalization, at a median of 6 days (lower-upper quartile, 4-10). Table 1 shows the baseline demographic, clinical,

laboratory and HRCT characteristics in the study group and also divided based on dead or alive status at discharge. HRCT was positive for interstitial pneumonia in 248 cases (89%).

Table 1

Comparing patients discharged alive with patients who died, the median (lower-upper quartiles) age was 65 y/o (56-76) vs 77 y/o (72-82), ($p<0.001$), n=95 (56%) vs n=74 (68%) were males, p=0.061, dyslipidemia was present in n=29 (17%) vs n=30 (28%), p=0.052, n=15 (9) vs n=26 (24), p=0.001 had prior cardiovascular disease, D-dimer median was 723 ng/ml (lower-upper quartile, 495-1119) vs 1.083 ng/ml (lower-upper quartile, 704-2248), $p<0.001$, CRP median 78.15 mg/L (lower-upper quartile, 36.8-132.5) vs 148.3 mg/L (lower-upper quartile, 91-209.4), $p<0.001$, median CCS was 17 (lower-upper quartile, 0-248) vs 188.7 (lower-upper quartile, 20.3-671.6), $p<0.001$ and the PCAT attenuation median was -76.4 HU (lower-upper quartile, -79.3, -76.6) vs -68.6 HU (lower-upper quartile, -75.9, -63.3), $p<0.001$. Figure 3 graphically shows the distribution of age, main laboratory and imaging variables according to the in-hospital outcome. Increased heart rate (>100 beats per minute) was found during HRCT scan in 46 (27%) of the discharged-alive patients and in 22 (20%) patients who died in hospital (p=0.245).

Figure 3

Table 2 (left column), shows available demographic, clinical, laboratory and HRCT characteristics, including the CCS and PCAT attenuation, tested with simple univariable logistic regression. The following variables were significantly associated with the end point: age (OR 1.073, 95%CI 1.05-1.10, $p<0.001$), male sex (OR 1.67, 95%CI 1.0-2.76, p=0.046), dyslipidemia (OR 1.85, 95%CI 1.03-3.30, p=0.038), prior cardiovascular disease (OR 3.27, 95%CI 1.63-6.45, p=0.001), D-

dimer (OR 1.95. 95%CI 1.45-2.63, p<0.001), CRP (OR 2.12, 95%CI 1.55-2.92, p<0.001), HRCT extent of diseased lung parenchyma (OR 2.11, 95%CI 1.60-2.78, p<0.001), CCS (OR 1.27, 95% CI 1.14-1.39, p<0.001) and PCAT attenuation (increase per 5 HU, OR 1.53, 95%CI 1.31-1.79, p<0.001). First a multivariable logistic regression model comprising clinical and laboratory variables was created (Table 2 central column), then the HRCT variables were added in a second model (Table 2 right column). This last model showed that age (OR 1.07, 95%CI 1.04-1.11, p<0.001), D-dimer (OR 1.48, 95% CI 1.02-2.16, p=0.041), CRP (OR 1.81, 95%CI 1.25-2.61, p=0.002), percentage of affected lung parenchyma (OR 1.68, 95%CI 1.20-2.35, p=0.002) and PCAT attenuation (OR 1.58, 95%CI 1.30-1.91, p<0.001) were finally significantly associated with in-hospital mortality. For the sake of completeness we also report the final multivariable model after the variable age was removed due to the moderate but significant collinearity (Spearman's rho =0.557, p<0.001) with CCS (online appendix, Table A), instead of maintaining both variables as in Table 1.

Table 2

The first model with clinical+laboratory variables showed a receiver-operating-characteristic (ROC) curve area of 0.808 (95%CI 0.756-0.859), which was significantly increased by the addition of HRCT variables to the model, with a resulting ROC area of 0.861 (95%CI 0.817-0.905), p=0.004.

Figure 4 shows the comparison between two paradigmatic cases, one with lower PCAT attenuation indicating no coronary inflammation, and the other one showing higher PCAT attenuation (closer to 0 HU), indicating coronary inflammation.

Figure 4

Discussion

Peri-coronary adipose tissue attenuation, which correlates with coronary artery inflammation, was independently associated with in-hospital mortality in COVID-19 patients, as it was also the case for age, D-dimer, CRP and extent of diseased lungs on HRCT.

Coronary artery calcium, measured in the HRCT scans as a proxy for pre-existent subclinical coronary artery disease, was not associated on multivariable analysis with the primary end point of mortality, at least when the collinear variable age was kept in the model; this apparently reduces the odds that the cardiac contribution to increased mortality in COVID-19 patients is mediated by a demand-supply mismatch mechanism, caused by pre-existent CAD.

The semi-quantitative assessment of lung disease, a simple HRCT estimate available in real-time by the radiologist in charge was significantly and independently associated with mortality. Coronary inflammation was assessed using the recently described PCAT attenuation variable, a non-invasive volumetric measurement of x-ray attenuation of the adipose tissue in direct, close contact with the coronary arteries, which is an indirect “thermometer” of coronary inflammation (10, 15-17). Figure 3 shows the output PCAT attenuation images of a comparison between two paradigmatic, opposite cases.

Potential Cardiac Mechanisms Underlying Increased Mortality

Before the results of the current study we could not exclude that the prolonged hypoxemia typical of symptomatic COVID-19 represented a stress condition leading to myocardial injury, particularly in the elderly patients with asymptomatic CAD, through a demand-supply mismatch. Since the CCS is able to indirectly measure pre-existent CAD burden, and it was not independently associated with in-hospital death, we may reasonably conclude that pre-existent (known or unknown) CAD has no or limited role in worsening the outcome of COVID-19 patients. The

finding that a higher coronary inflammation status in COVID-19 patients is associated with mortality is instead a novel finding and may shed some light on the possible mechanisms responsible for the frequently-found myocardial injury, associated with higher mortality in COVID-19 patients (4-7). However, the current study did not address the incidence of myocardial injury because cardiac troponins were not routinely measured in our COVID-19 cohort, so that while we can affirm that coronary inflammation is associated with in-hospital death, we cannot speculate on the relation between coronary inflammation and myocardial injury. The finding of a disproportionate increase in CRP, together with higher PCAT attenuation in patients with fatal outcome, supports the existing hypothesis that inflammation in COVID-19 is a key driver of outcome, being a possible mechanism of coronary plaque destabilization, as well as a potential trigger for cardiac arrhythmias (18). This opens the possibility that the potent anti-inflammatory drugs already in testing phase in prospective trials may help decrease mortality.

COVID-19 diagnosis by viral nucleic acid isolation or radiologically by HRCT and the Bayes theorem

Although the demonstration of SARS-CoV-2 nucleic acid in the nasopharyngeal swab remains the reference for COVID-19 diagnosis (12), it has several limitations, which may limit its diagnostic sensitivity to lower than ideal. The use of HRCT as an initial gatekeeper, as performed in the current study in presence of symptoms and signs suggestive of the disease, may prove useful during massive outbreaks, as the one the world is facing. In an outbreak setting the inherently limited specificity of HRCT – which aims at the detection of a typical interstitial pneumonia, and not specifically at the detection of the virus – is sufficient to produce a moderate-to-high positive predictive value, due to the high prevalence of disease and high pre-test probability. In turn, HRCT has a very high sensitivity and negative predictive value, which may be preferable in the gatekeeping setting of highly contagious diseases (19).

COVID-19 prognosis by HRCT

The current study also demonstrated that HRCT is capable to accurately risk-stratify patients with acute respiratory distress and laboratory-confirmed COVID-19 through simple semi-quantitative estimation of the extent of lung parenchyma affected by pneumonia, which represents the pulmonary key clinical manifestation of COVID-19. Interestingly, such risk-stratification capability, although to a lesser degree, was demonstrated also in patients in whom viral nucleic acid was not detected in at least two nasopharyngeal swabs (Figure 2). Whether this is due to RT-PCR on swabs being insufficiently sensitive or to HRCT being able to stratify also non-COVID-19 patients would require an independent reference method for COVID-19 disease, which is not available at this time.

Limitations

Our study has limitations. First, we cannot unequivocally classify those patients with HRCT findings typical of COVID-19 who tested negative to viral nucleic acid detection in nasopharyngeal swabs, since the direct virus detection remains the WHO recommended standard for COVID-19 diagnosis (12). The mounting clinical experience during the outbreak suggests that most such patients may be affected by COVID-19, since the nasopharyngeal detection of the virus is limited in sensitivity and the optimal timing to perform the swab unknown. Second, as a retrospective study, specific information regarding the prevalence of optional variables, for example the presence of myocardial injury by high-sensitivity troponins, were not available, owing to the difficult clinical conditions in the isolation wards and the urgency of containing the epidemic. Another limitation was that the presence of obesity was adjudicated as a binary variable by the caring physicians (body mass index>29 kg/m2), but individual granular data are not available.

Third, though the methods used to calculate the CCS in non-contrast and non ECG-triggered HRCT scans have been previously validated (11,20,21), the HRCT protocol is not the gold-standard to measure the CCS, and this scan protocol has never been used previously for the measurement of PCAT attenuation. To our knowledge, ours is the first study to report such PCAT attenuation measurement and its clinical results. The absolute value of fat attenuation in Hounsfield units might potentially differ between an ideal ECG-triggered and contrast computed tomography angiogram and a non-contrast, non-ECG triggered HRCT as available in the current study, although a good correlation of between PCAT measurement is now documented between precontrast and postcontrast scans (22). However, since all patients underwent the same modality of HRCT scans, the relative comparison between alive and dead patients in our study should be unbiased by this limitation, even more considering there was no difference in the number of patients with an increased heart rate (>100 beats per minute, table 1) which in theory could lead to partial volume effect of coronary artery lumen and its surroundings. Further we measured PCAT attenuation only in one coronary artery (LAD), because it was the one technically best visualized (most stable) in the given conditions of HRCT scans. Prior literature robustly supports that PCAT attenuation does not differ significantly among coronary arteries in a given individual, and right coronary artery or LAD may be used alternatively as inflammatory markers of overall coronary inflammatory status (15-17).

Conclusions

While the current study confirms prior data that increased age, D-dimer and CRP are associated with in-hospital mortality in COVID-19, we also report that the simple extent of lung disease and the novel PCAT attenuation parameter of coronary artery inflammation in HRCT scans are also independently associated with mortality. This may hypothetically lend support to therapeutic strategies aimed at lowering inflammation during COVID-19, which would possibly exert their positive effects also on the inflamed coronary arteries.

Funding: No funding was required for this research work.

References

1) Guan WJ, Ni ZY, Hu Y, Liang WH, Ou CQ, He JX, Liu L, Shan H, Lei CL, Hui DSC, Du B, Li LJ, Zeng G, Yuen KY, Chen RC, Tang CL, Wang T, Chen PY, Xiang J, Li SY, Wang JL, Liang ZJ, Peng YX, Wei L, Liu Y, Hu YH, Peng P, Wang JM, Liu JY, Chen Z, Li G, Zheng ZJ, Qiu SQ, Luo J, Ye CJ, Zhu SY, Zhong NS, China Medical Treatment Expert Group for C. Clinical Characteristics of Coronavirus Disease 2019 in China. N Engl J Med 2020;**382**(18):1708-1720.
2) Wu Z, McGoogan JM. Characteristics of and Important Lessons From the Coronavirus Disease 2019 (COVID-19) Outbreak in China: Summary of a Report of 72314 Cases From the Chinese Center for Disease Control and Prevention. JAMA 2020..
3) Onder G, Rezza G, Brusaferro S. Case-Fatality Rate and Characteristics of Patients Dying in Relation to COVID-19 in Italy. JAMA 2020..
4) Bonow RO, Fonarow GC, O'Gara PT, Yancy CW. Association of Coronavirus Disease 2019 (COVID-19) With Myocardial Injury and Mortality. JAMA Cardiol 2020..
5) Shi S, Qin M, Shen B, Cai Y, Liu T, Yang F, Gong W, Liu X, Liang J, Zhao Q, Huang H, Yang B, Huang C. Association of Cardiac Injury With Mortality in Hospitalized Patients With COVID-19 in Wuhan, China. JAMA Cardiol 2020.
6) Guo T, Fan Y, Chen M, Wu X, Zhang L, He T, Wang H, Wan J, Wang X, Lu Z. Cardiovascular Implications of Fatal Outcomes of Patients With Coronavirus Disease 2019 (COVID-19). JAMA Cardiol 2020.
7) Zheng YY, Ma YT, Zhang JY, Xie X. COVID-19 and the cardiovascular system. Nat Rev Cardiol 2020;**17**(5):259-260.

8) Inciardi RM, Lupi L, Zaccone G, Italia L, Raffo M, Tomasoni D, Cani DS, Cerini M, Farina D, Gavazzi E, Maroldi R, Adamo M, Ammirati E, Sinagra G, Lombardi CM, Metra M. Cardiac Involvement in a Patient With Coronavirus Disease 2019 (COVID-19). JAMA Cardiol 2020.

9) Wang M, Liu Y, Zhou X, Zhou J, Zhang H, Zhang Y. Coronary calcium score improves the estimation for pretest probability of obstructive coronary artery disease and avoids unnecessary testing in individuals at low extreme of traditional risk factor burden: validation and comparison of CONFIRM score and genders extended model. BMC Cardiovasc Disord 2018;**18**(1):176.

10) Antonopoulos AS, Sanna F, Sabharwal N, Thomas S, Oikonomou EK, Herdman L, Margaritis M, Shirodaria C, Kampoli AM, Akoumianakis I, Petrou M, Sayeed R, Krasopoulos G, Psarros C, Ciccone P, Brophy CM, Digby J, Kelion A, Uberoi R, Anthony S, Alexopoulos N, Tousoulis D, Achenbach S, Neubauer S, Channon KM, Antoniades C. Detecting human coronary inflammation by imaging perivascular fat. Sci Transl Med 2017;**9**(398).

11) Budoff MJ, Nasir K, Kinney GL, Hokanson JE, Barr RG, Steiner R, Nath H, Lopez-Garcia C, Black-Shinn J, Casaburi R. Coronary artery and thoracic calcium on noncontrast thoracic CT scans: comparison of ungated and gated examinations in patients from the COPD Gene cohort. J Cardiovasc Comput Tomogr 2011;**5**(2):113-8.

12) WHO. Clinical management of severe acute respiratory infection when novel coronavirus (nCoV) infection is suspected: interim guidance. https://apps.who.int/iris/handle/10665/330854 (30 March 2020)

13) Scott S, Kay FU, Abbara S, et al. Radiological Society of North America Expert Consensus Statement on Reporting Chest CT Findings Related to COVID-19. Endorsed by the Society

of Thoracic Radiology, the American College of Radiology, and RSNA. Radiology: Cardiothoracic imaging 2020.

14) Agatston AS, Janowitz WR, Hildner FJ, Zusmer NR, Viamonte M, Jr., Detrano R. Quantification of coronary artery calcium using ultrafast computed tomography. J Am Coll Cardiol 1990;**15**(4):827-32.

15) Kwiecinski J, Dey D, Cadet S, Lee SE, Otaki Y, Huynh PT, Doris MK, Eisenberg E, Yun M, Jansen MA, Williams MC, Tamarappoo BK, Friedman JD, Dweck MR, Newby DE, Chang HJ, Slomka PJ, Berman DS. Peri-Coronary Adipose Tissue Density Is Associated With (18)F-Sodium Fluoride Coronary Uptake in Stable Patients With High-Risk Plaques. JACC Cardiovasc Imaging 2019;**12**(10):2000-2010.

16) Gaibazzi N, Martini C, Botti A, Pinazzi A, Bottazzi B, Palumbo AA. Coronary Inflammation by Computed Tomography Pericoronary Fat Attenuation in MINOCA and Tako-Tsubo Syndrome. J Am Heart Assoc 2019;**8**(17):e013235.

17) Oikonomou EK, Marwan M, Desai MY, Mancio J, Alashi A, Hutt Centeno E, Thomas S, Herdman L, Kotanidis CP, Thomas KE, Griffin BP, Flamm SD, Antonopoulos AS, Shirodaria C, Sabharwal N, Deanfield J, Neubauer S, Hopewell JC, Channon KM, Achenbach S, Antoniades C. Non-invasive detection of coronary inflammation using computed tomography and prediction of residual cardiovascular risk (the CRISP CT study): a post-hoc analysis of prospective outcome data. Lancet 2018;**392**(10151):929-939.

18) Lazzerini PE, Boutjdir M, Capecchi PL. COVID-19, Arrhythmic Risk and Inflammation: Mind the Gap! Circulation 2020.

19) Ai T, Yang Z, Hou H, Zhan C, Chen C, Lv W, Tao Q, Sun Z, Xia L. Correlation of Chest CT and RT-PCR Testing in Coronavirus Disease 2019 (COVID-19) in China: A Report of 1014 Cases. Radiology 2020:200642.

20) Xie X, Zhao Y, de Bock GH, de Jong PA, Mali WP, Oudkerk M, Vliegenthart R. Validation and prognosis of coronary artery calcium scoring in nontriggered thoracic computed tomography: systematic review and meta-analysis. Circ Cardiovasc Imaging 2013;**6**(4):514-21.

21) van Velzen SGM, Lessmann N, Velthuis BK, et al. Deep Learning for Automatic Calcium Scoring in CT: Validation Using Multiple Cardiac CT and Chest CT Protocols. Radiology. 2020;295(1):66–79.

22) Almeida S, Pelter M, Shaik K et al. Feasibility of Measuring Pericoronary Fat from Precontrast Scans: Effect of Iodinated Contrast on Pericoronary Fat Attenuation. Journal of Cardiovascular Computed Tomography. Article in press. https://doi.org/10.1016/j.jcct.2020.04.004

1 23)

2 **Table 1.** Demographics, Clinical, Laboratory tests and HRCT Characteristics of Patients

3 With laboratory-confirmed COVID-19.

	Total	Alive at discharge	Dead	P value
Demographics				
No of patients	279	170 (61)	109 (39)	
Time to death (lower-upper quartile)	-	-	6 (4-10)	-
Age, median (lower-upper quartile), y	72 (60-80)	65 (56-76)	77 (72-82)	0.000
Male sex	169 (61)	95 (56)	74 (68)	0.061
Risk factors and patient history				
Hypertension	157 (56)	92 (54)	65 (60)	0.434
Hypercholesterolemia	59 (21)	29 (17)	30 (28)	0.052
Current Smoker	10 (4)	5 (3)	5 (5)	0.695
Diabetes mellitus	60 (22)	32 (19)	28 (26)	0.225
Prior cardiovascular disease	41 (15)	15 (9)	26 (24)	0.001
Obesity	29 (16)	13 (8)	16 (15)	0.09
Laboratory blood tests				

CRP[a], median (lower-upper quartile) mg/L	104 (46-164)	78.15 (36.8-132.5)	148.3 (91-209.4)	0.000
D-Dimer, median (lower-upper quartile) ng/ml	832 (580-1427)	723 (495-1119)	1.083 (704-2248)	0.000
HRCT[b]				
Increased heart rate during HRCT (>100 beats per minute)	68 (24)	46 (27)	22 (20)	0.245
Positive	248 (89)	155 (91)	93 (85%)	0.186
Negative	13 (4)	8 (5)	4 (4)	0.910
Indeterminate	19 (7)	7 (4)	12 (11)	0.047
Lung involvement [c], (visual %)				
>80%	18 (6)	5 (3)	13 (12)	0.006
50-80%	66 (24)	26 (15)	40 (37)	0.000
20-49%	110 (39)	70 (41)	40 (37)	0.534
10-19%	59 (21)	49 (29)	10 (9)	0.000
<10%	26 (9)	20	6 (5)	0.123
Agatston coronary calcium score, (lower-upper quartile)	73 (0-382)	17 (0-248)	188.7 (20.3-671.6)	0.000
PCAT [d] attenuation LAD [e], (lower-upper quartile) HU [f]	-74.9 (-78.7 -67.5)	-76.4 (-79.3 -76.6)	-68.6 (-75.9- -63.3)	0.000

No. (%, if not otherwise specified)

[a] CRP, C-reactive protein

[b] HRCT, High Resolution Computed Tomography

[c] independently from positive, negative or indeterminate for signs of interstitial pneumonia

[d] PCAT, peri-coronary adipose tissue attenuation

[e] LAD, left anterior descending artery

[f] HU, Hounsfield Units

Table 2. Relationship of clinical factors, serum biomarkers, and CT assessment (lungs, heart and peri-coronary adipose tissue) with in-hospital death

In-hospital death						
Univariable analysis			Multivariable analysis			
	OR (95% CI)	p-value	Model 1 [a] OR (95% CI)	p-value	Model 2 [b] OR (95% CI)	p-value
Age	1.07 (1.05-1.10)	<0.001	1.07 (1.04-1.10)	<0.001	1.07 (1.04-1.11)	<0.001
Male sex	1.67 (1.0-2.76)	0.046	-	-	-	-
Hypertension	1.25 (0.77-2.04)	0.365	-	-	-	-
Dyslipidemia	1.85 (1.03-3.30)	0.038	-	-	2.04 (0.96-4.34)	0.064
Current Smoker	0.77 (0.51-1.17)	0.230	-	-	-	-
Diabetes mellitus	1.49 (0.84-2.65)	0.175	-	-	-	-
Prior CV [c] disease	3.27 (1.63-6.45)	0.001	-	-	-	-
Obesity	2.08 (0.96-4.51)	0.065	2.55 (1.03-6.33)	0.043	-	-
D-dimer	1.95 (1.45-2.63)	<0.001	1.53 (1.09-2.15)	0.013	1.48 (1.02-2.16)	0.041
C-reactive protein	2.12 (1.55-2.92)	<0.001	2.02 (1.43-2.84)	<0.001	1.81 (1.25-2.61)	0.002
% affected lung parenchyma	2.11 (1.60-2.78)	<0.001			1.68 (1.20-2.35)	0.002
Agatston coronary calcium score	1.266 (1.14-1.39)	<0.001			-	-
PCAT [d] attenuation, HU [e]	1.53 (1.31-1.79)	<0.001			1.58 (1.30-1.91)	<0.001

[a] Clinical + laboratory

[b] Clinical + laboratory + high resolution computed tomography

[c] CV, Cardiovascular

[d] PCAT, peri-coronary adipose tissue attenuation

[e] HU, Hounsfield Units

Figure legends

Figure 1. Identification of the left anterior descending coronary artery from HRCT dataset, manual tracing of the vessel course and, finally, peri-coronary fat attenuation measurement.

HRCT, high-resolution computed tomography.

Figure 2. Histograms describing mortality rate in groups classified based on HRCT results or SARS-CoV-2 PCR assay results and also histograms describing mortality rates based on visual estimate of the percentage lung parenchyma diseased, either in COVID-19 laboratory-confirmed patients or not.

HRCT, high-resolution computed tomography.

Figure 3. Distribution of age, D-dimer and CRP values, and imaging data acquired from HRCT, based on primary outcome of in-hospital death.

CRP, C-reactive protein; HRCT, high-resolution computed tomography.

Figure 4. Comparison between the PCAT attenuation assessment in a COVID-19 patient with more inflamed LAD coronary artery (left panel, same patient shown in figure 1) and another COVID-19 patient with less inflamed LAD coronary artery (right panel).

PCAT, peri-coronary adipose tissue; LAD, left anterior descending.

Figure 1.

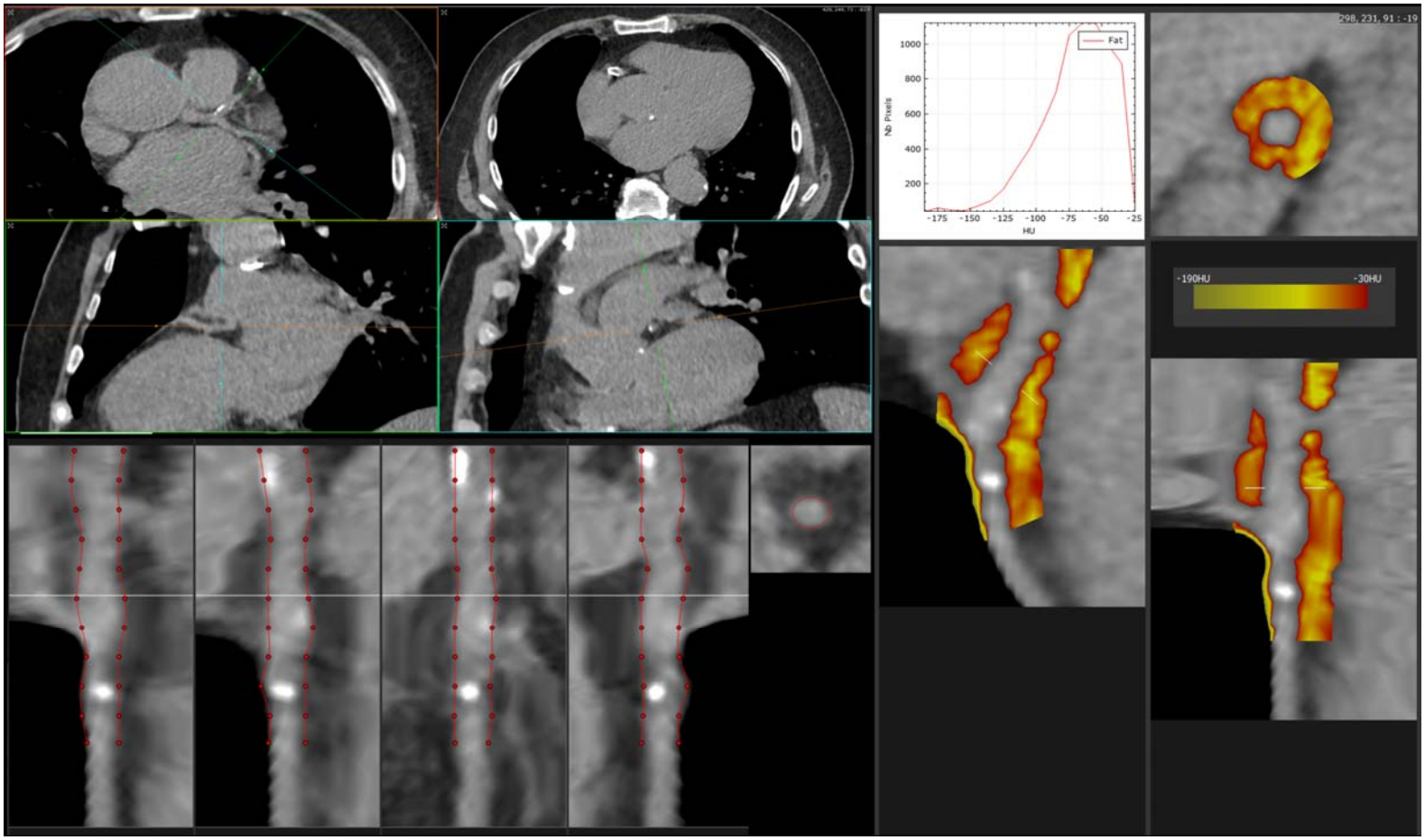

Figure 2.

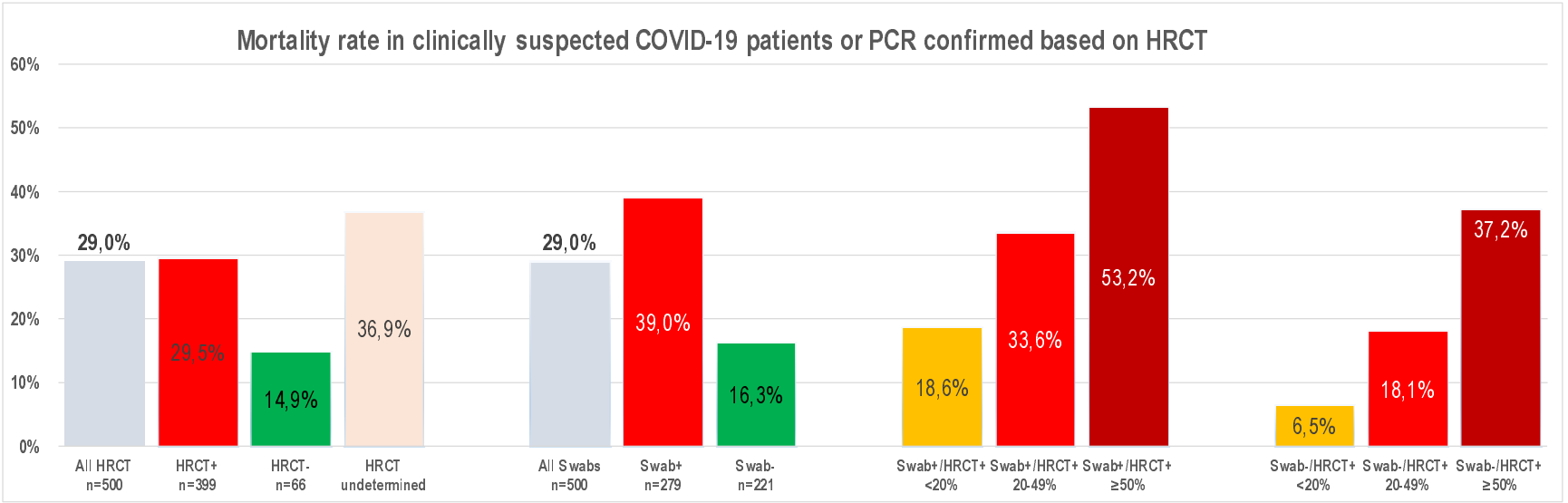
Mortality rate in clinically suspected COVID-19 patients or PCR confirmed based on HRCT
60%
50%
40%
30%
20%
10%
0%
29,0%
29,5%
14,9%
36,9%
29,0%
39,0%
16,3%
18,6%
33,6%
53,2%
6,5%
18,1%
37,2%
All HRCT n=500
HRCT+ n=399
HRCT- n=66
HRCT undetermined
All Swabs n=500
Swab+ n=279
Swab- n=221
Swab+/HRCT+ <20%
Swab+/HRCT+ 20-49%
Swab+/HRCT+ ≥50%
Swab-/HRCT+ <20%
Swab-/HRCT+ 20-49%
Swab-/HRCT+ ≥50%

Figure 3.

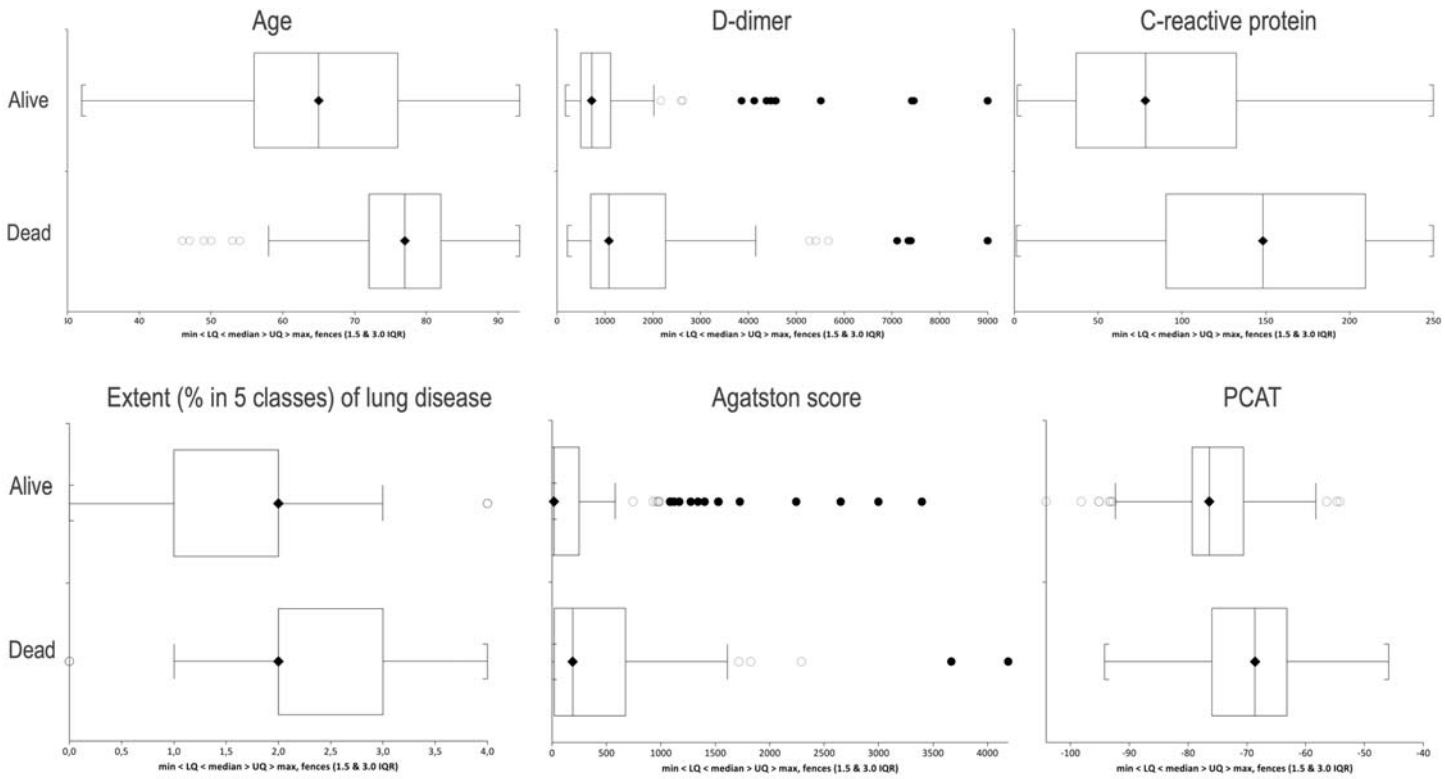
Age
Alive
Dead
40
50
60
70
80
90
min < LQ < median > UQ > max, fences (1.5 & 3.0 IQR)
D-dimer
0
1000
2000
3000
4000
5000
6000
7000
8000
9000
min < LQ < median > UQ > max, fences (1.5 & 3.0 IQR)
C-reactive protein
0
50
100
150
200
250
min < LQ < median > UQ > max, fences (1.5 & 3.0 IQR)
Extent (% in 5 classes) of lung disease
Alive
Dead
0,0
0,5
1,0
1,5
2,0
2,5
3,0
3,5
4,0
min < LQ < median > UQ > max, fences (1.5 & 3.0 IQR)
Agatston score
0
500
1000
1500
2000
2500
3000
3500
4000
min < LQ < median > UQ > max, fences (1.5 & 3.0 IQR)
PCAT
-100
-90
-80
-70
-60
-50
-40
min < LQ < median > UQ > max, fences (1.5 & 3.0 IQR)

Figure 4.

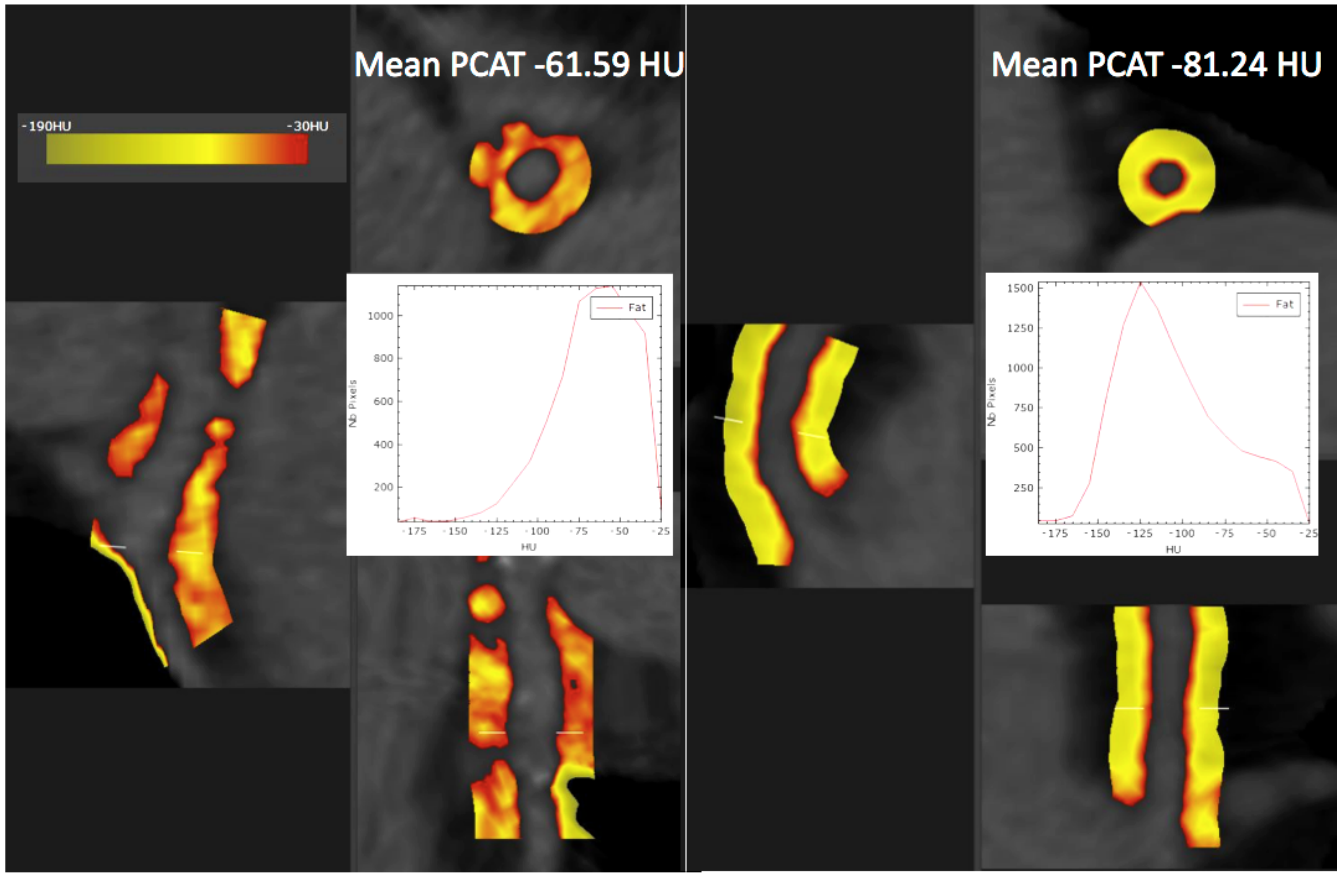
-190HU
-30HU
Mean PCAT -61.59 HU
Fat
Nb Pixels
HU
Mean PCAT -81.24 HU
Fat
Nb Pixels
HU

Take-home figure

Comparison between the left anterior descending peri-coronary adipose tissue (LAD-PCAT) attenuation in two COVID-19 patients, the first showing higher vessel inflammation (left panel) compared to the second (right panel). Coronary artery inflammation measured by PCAT attenuation – not coronary calcium score – is significantly associated with higher mortality in COVID-19 patients.